

Ph.D. Dissertation

b-제트 안의 참 쿼크 중간자를 이용한 탑 쿼크  
질량 측정  
Top quark mass measurement using  
charmed meson within b-jet

by

Geonmo Ryu

Department of Physics

The Graduate School of the University of Seoul

February 2017

# Top quark mass measurement using charmed meson within b-jet

by  
Geonmo Ryu

A Ph.D. Dissertation submitted to the  
Department of Physics at the Graduate School  
of the University of Seoul in partial fulfillment  
of the requirements for the degree of Doctor of  
Philosophy

December 2016

Approved by  
Inkyu Park  
Advisor

**This certifies that Ph.D. dissertation of  
Geonmo Ryu is approved.**

---

**Thesis Committee Chair:** Hyunsoo Min

---

**Thesis Committee Member:** Inkyu Park

---

**Thesis Committee Member:** Jason Lee

---

**Thesis Committee Member:** Intae Yu

---

**Thesis Committee Member:** Tae Jeong Kim

**The Graduate School of the University of Seoul**

**February 2017**

## Abstract

# Top quark mass measurement using charmed meson within b-jet

Geonmo Ryu

Department of Physics

The Graduate School

University of Seoul

To measure top quark mass by using charmed mesons from b quark jet is presented as an alternative solution among various top quark mass measurement. This method has a merit about the jet energy uncertainty because it did not use jet's energy directly. Particularly, we focus on charmed mesons of b-jets like as  $D^0$ ,  $D^*(2010)$  and  $J/\psi$  on this thesis. These mesons can be decayed to charged hadrons or leptons instead of neutral particles. So, this property can minimize a noise effect from background and pileup energy. Using Run2016  $L = 15.9\text{fb}^{-1}\sqrt{s} = 13\text{TeV}$  events at CMS detector, we confirmed that the invariant mass of isolated lepton and the charmed meson has a correlation with top quark mass. In addition, we extracted top quark mass from calibration curve of  $M_{top}$  vs  $M_{l+sv}$ . Using  $l + D^0$  meson, we acquired the top mass as  $180.69 \pm 5.73$  (stat.)  $^{+9.61}_{-8.67}$  (syst.)  $\text{GeV}/c^2$ .

Unfortunately,  $J/\psi$  and  $D^*(2010)$  can not be fitted due to too small statistic.

Ph.D. Dissertation

b-제트 안의 참 쿼크 중간자를 이용한 탑 쿼크  
질량 측정  
Top quark mass measurement using  
charmed meson within b-jet

by

Geonmo Ryu

Department of Physics

The Graduate School of the University of Seoul

February 2017

# Table of Contents

<b>Abstract</b>	<b>4</b>
<b>Table of Content</b>	<b>i</b>
<b>List of Figures</b>	<b>v</b>
<b>List of Tables</b>	<b>vii</b>
<b>1 Introduction</b>	<b>1</b>
<b>2 Theoretical overview</b>	<b>3</b>
2.1 Standard Model . . . . .	3
2.1.1 Quantum Chromodynamics (QCD) . . . . .	5
2.2 Top and anti-Top ( $t\bar{t}$ ) pair production at 13TeV . . . . .	5
2.2.1 ElectroWeak interaction . . . . .	5
2.2.2 Decay channel of $t\bar{t}$ event . . . . .	5
2.2.3 Charmed mesons from b quark jet . . . . .	5

TABLE OF CONTENTS

<b>3</b>	<b>Previous measurement of top quark mass</b>	<b>6</b>
3.1	Mass measurement from Tevatron . . . . .	6
3.1.1	Result from Tevatron . . . . .	6
3.2	Mass measurement from LHC . . . . .	6
3.2.1	Combination results from LHC . . . . .	6
3.2.2	Similar method results . . . . .	7
<b>4</b>	<b>Experimental Setup</b>	<b>8</b>
4.1	Large Hadron Collider(LHC) . . . . .	8
4.1.1	CMS Detector . . . . .	8
4.1.1.1	Tracker . . . . .	8
4.1.1.2	Electromagnetic Calorimeter(HCAL) . . . . .	8
4.1.1.3	Hadron Calorimeter(ECAL) . . . . .	8
4.1.1.4	Muon System . . . . .	8
<b>5</b>	<b>Computing</b>	<b>9</b>
5.1	GRID Computing for LHC experiment . . . . .	9
5.1.1	LHC Computing Grid(LCG) . . . . .	9
5.1.2	Middleware . . . . .	10
5.1.3	Dataset and Data Aggregation System . . . . .	10
5.1.4	SRM protocol and ROOT FileSystem . . . . .	10
5.1.5	PhEDEx : Large Size File Transfer System . . . . .	10



TABLE OF CONTENTS

5.2	System Setup . . . . .	10
<b>6</b>	<b>Physics object reconstruction</b>	<b>11</b>
6.1	Muon . . . . .	11
6.2	Electron . . . . .	12
6.3	ParticleFlow(PF) algorithm . . . . .	14
6.3.1	Charged Hadron, Neutral Hadron and Photon . . . . .	14
6.4	Jet . . . . .	15
6.4.1	b-tagging . . . . .	15
6.5	Missing ET . . . . .	16
<b>7</b>	<b>Reconstruction of the charmed mesons</b>	<b>17</b>
7.1	Track Selection . . . . .	17
7.1.1	Kalman vertex fitter . . . . .	18
7.2	Reconstruction of charmed meson . . . . .	18
7.2.1	$J/\psi$ . . . . .	18
7.2.2	$D^0$ . . . . .	19
7.2.3	$D^*(2010)$ . . . . .	21
<b>8</b>	<b>Top quark mass measurement</b>	<b>23</b>
8.1	Monte Carlo Samples . . . . .	23
8.2	Collision Data . . . . .	24

## TABLE OF CONTENTS

8.3	Event Selection . . . . .	26
8.3.1	Object selection . . . . .	27
8.3.1.1	Muon . . . . .	27
8.3.1.2	Electron . . . . .	27
8.3.1.3	Jet . . . . .	27
8.3.2	Kinematic selection . . . . .	28
8.4	Systematic Errors . . . . .	30
8.5	Result . . . . .	33
8.5.1	Fast Simulation result for toy $100fb^{-1}$ . . . . .	33
8.5.2	Full Simulation result for Run2016 . . . . .	33
<b>9</b>	<b>Conclusion</b>	<b>39</b>
	<b>Reference</b>	<b>41</b>

# List of Figures

2.1	Elementary particles of the standard model . . . . .	4
2.2	Tree-level LO Feynman diagrams that contribute to $t\bar{t}$ production.	5
6.1	Overview to reconstruction of PF Electron . . . . .	13
7.1	Various muon reconstruction candidates properties and $J/\psi$ mass distribution . . . . .	20
7.2	$D^0$ Candidates invariant mass distribution . . . . .	21
7.3	$D^*$ Candidates invariant mass and difference mass distribution . . .	22
8.1	Reconstructed charmed meson mass distribution . . . . .	33
8.2	$M_{l+J/\psi}^{inv.}$ with Gaussian fitting . . . . .	34
8.3	$l + D^0 + l$ with Gaussian fitting . . . . .	35
8.4	$l + D^*(2010) + l$ with Gaussian fitting . . . . .	36
8.5	Calibration curve for fast simulation $\mathcal{L} = 100fb^{-1}$ at $\sqrt{s} = 13TeV$ .	37
8.6	$l + D^0$ with landau fitting . . . . .	37

## LIST OF FIGURES

8.7 Calibration curve for full simulation  $\mathcal{L} = 15.9fb^{-1}$  at  $\sqrt{s} = 13TeV$  . 38

# List of Tables

8.1	Monte Carlo dataset list . . . . .	25
8.2	Run2016 13TeV data $\mathcal{L} = 15.9fb^{-1}$ . . . . .	26
8.3	High Level Trigger information for each primary datasets . . . . .	26
8.4	Electron cut based medium ID . . . . .	28
8.5	Jet Loose ID . . . . .	28
8.6	Event Selection for dileptonic decay channel for ttbar signal sample.	29
8.7	The expected numbers of signal events and backgrounds after event selection . . . . .	30
8.8	Systematic errors for D0 case . . . . .	32

# Chapter 1

## Introduction

On Standard Model, a top quark is heaviest elementary particle. In addition, the top quark has largest mass uncertainty. Therefore, to measure top quark mass is valuable and can help to search beyond standard model or to precisely measure some particle's properties which decay into top quark. After discovery of top quark in 1995, many measurement were developed and improved. In recent years, for dileptonic decay channel, analytic solution was published and measured to precise top quark mass. However, this method has a limitation about jet energy uncertainty. As collision energy will go higher, the jet energy uncertainty also will increase due to background and pileup energy. So, we need to explore another solution to overcome this limitation. We proposed to measure top quark mass using charmed meson within b-jet. Because, this method did not use jet energy to re-

## CHAPTER 1. INTRODUCTION

construct top quark mass directly. so, we can minimized jet uncertainty effect for mass measurement.

## Chapter 2

# Theoretical overview

### 2.1 Standard Model

The Standard model is a theory to compile the three of four fundamental interactions at nature like as electromagnetic, weak and strong interactions except gravity. As Fig 2.1, this theory describes 12 flavor quarks and lepton include for each antiparticle, 4 kinds of interaction mediate bosons and higgs boson.[1] In theoretically, the model is consist of Electroweak theory, QCD and higgs mechanism. The QCD is a theory about strong interactions of between quarks and gluons. The electroweak theory explains about electromagnetic interaction for charged particles and weak interaction for left-handed fermion, W and Z gauge bosons. Then, the higgs mechanism explains how the fermions and gauge bosons obtained the masses.



CHAPTER 2. THEORETICAL OVERVIEW

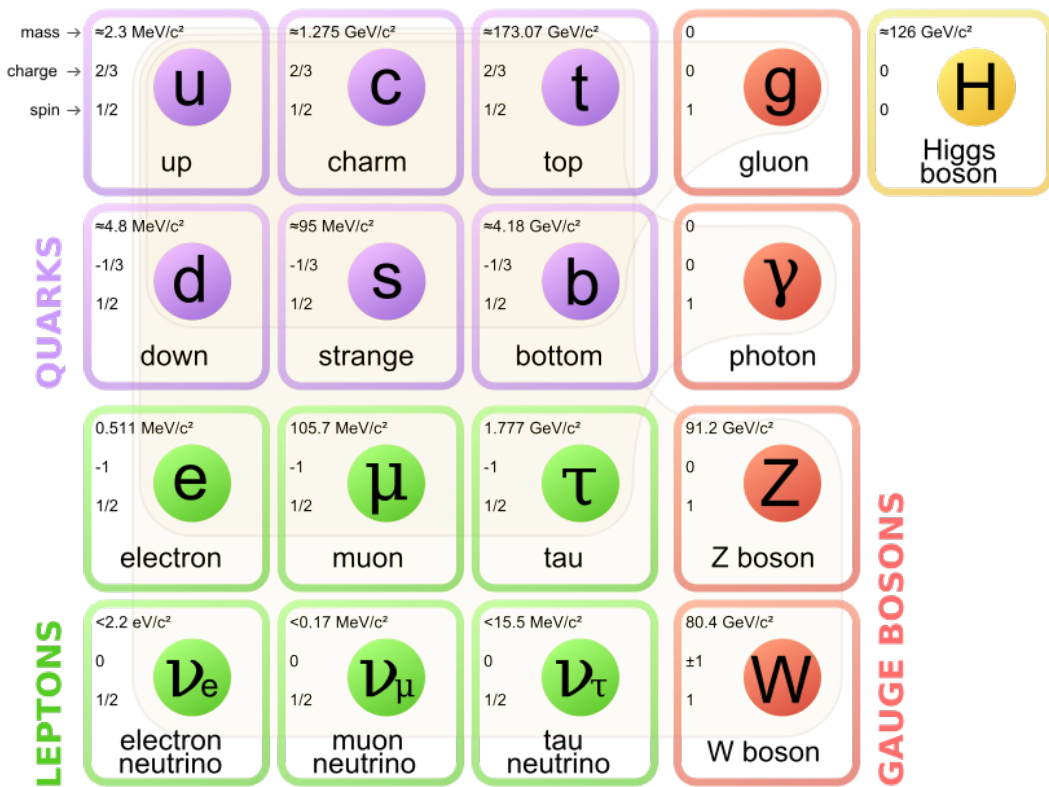


Figure 2.1: Elementary particles of the standard model

## CHAPTER 2. THEORETICAL OVERVIEW

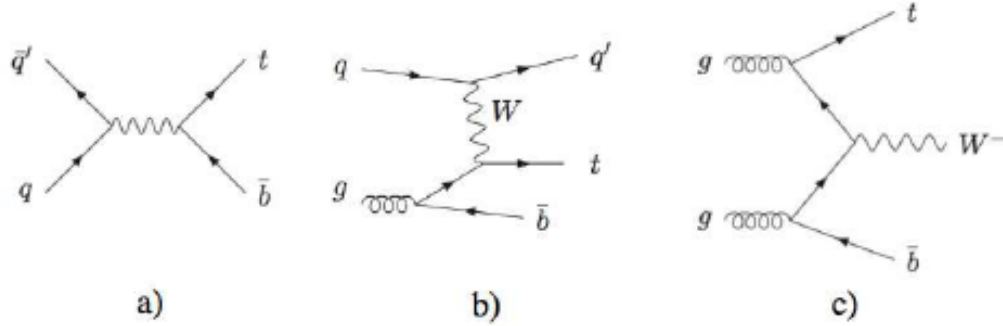


Figure 2.2: Tree-level LO Feynman diagrams that contribute to  $t\bar{t}$  production.

### 2.1.1 Quantum Chromodynamics (QCD)

Among the fermion particles, only quarks are affected by strong interaction. It means that they have a different quantum number as "color". This color has 3 types for each quark as red, green and blue.

## 2.2 Top and anti-Top ( $t\bar{t}$ ) pair production at 13TeV

On Fig2.2,[2]

### 2.2.1 ElectroWeak interaction

### 2.2.2 Decay channel of $t\bar{t}$ event

### 2.2.3 Charmed mesons from b quark jet

## Chapter 3

# Previous measurement of top quark mass

### 3.1 Mass measurement from Tevatron

#### 3.1.1 Result from Tevatron

mass :

### 3.2 Mass measurement from LHC

#### 3.2.1 Combination results from LHC

mass :

## CHAPTER 3. PREVIOUS MEASUREMENT OF TOP QUARK MASS

### 3.2.2 Similar method results

# Chapter 4

## Experimental Setup

### 4.1 Large Hadron Collider(LHC)

#### 4.1.1 CMS Detector

##### 4.1.1.1 Tracker

##### 4.1.1.2 Electromagnetic Calorimeter(HCAL)

##### 4.1.1.3 Hadron Calorimeter(ECAL)

##### 4.1.1.4 Muon System

- DT and CSC
- RPC and GEM

# Chapter 5

## Computing

### 5.1 GRID Computing for LHC experiment

#### 5.1.1 LHC Computing Grid(LCG)

The Collision data which are produced from CMS detector are too big by handle small size cluster. Thus, many computing resource were required to analysis. However, to buying and gathering resources into specific regions is not efficiency due to cost problem. So, GRID computing was developed to solve this problem.

## CHAPTER 5. COMPUTING

### 5.1.2 Middleware

### 5.1.3 Dataset and Data Aggregation System

### 5.1.4 SRM protocol and ROOT FileSystem

### 5.1.5 PhEDEx : Large Size File Transfer System

## 5.2 System Setup

## Chapter 6

# Physics object reconstruction

On feymann diagram of  $t\bar{t}$  event, we will find various objects as stable particles like as the leptons, Jets and MET(neutrino) to select event or measure top quark mass. It mean that we need to know how to assign a particle candidate to proper physics object.

### 6.1 Muon

A muon has a proper mass(100MeV) to pass though the ECAL and the HCAL. So, we can measure the muon hits from the tracker to muon system which located at calorimeter's outside. We have 3 muon categories which are proposed by CMS Muon Physics object Group(POG).[3]

1. Standalone Muon : This standalone muons are reconstructed using only hits



## CHAPTER 6. PHYSICS OBJECT RECONSTRUCTION

which are located at muon system. Due to no link to any other sub detector, the standalone muons may have a large identification rate.

2. Global Muon(Outside-in) : If a standalone muon can link to a tracker's track, it will be assigned as global muon. Because this global muon used whole information of muon system and tracker, it will be the best muon candidates.
3. Tracker Muon(Inside-out) : If a tracker track can link to a muon segment of muon system, it will be assigned as a tracker muon. It did not use full muon system information. So, it may be a fake muon. However, it don't need to fulfill standalone muon. It means that some tracks can be kept which don't have enough momentum. On this study, we need to find non-isolated soft leptons within jet. In this case, this tracker muon can be considerable.

### 6.2 Electron

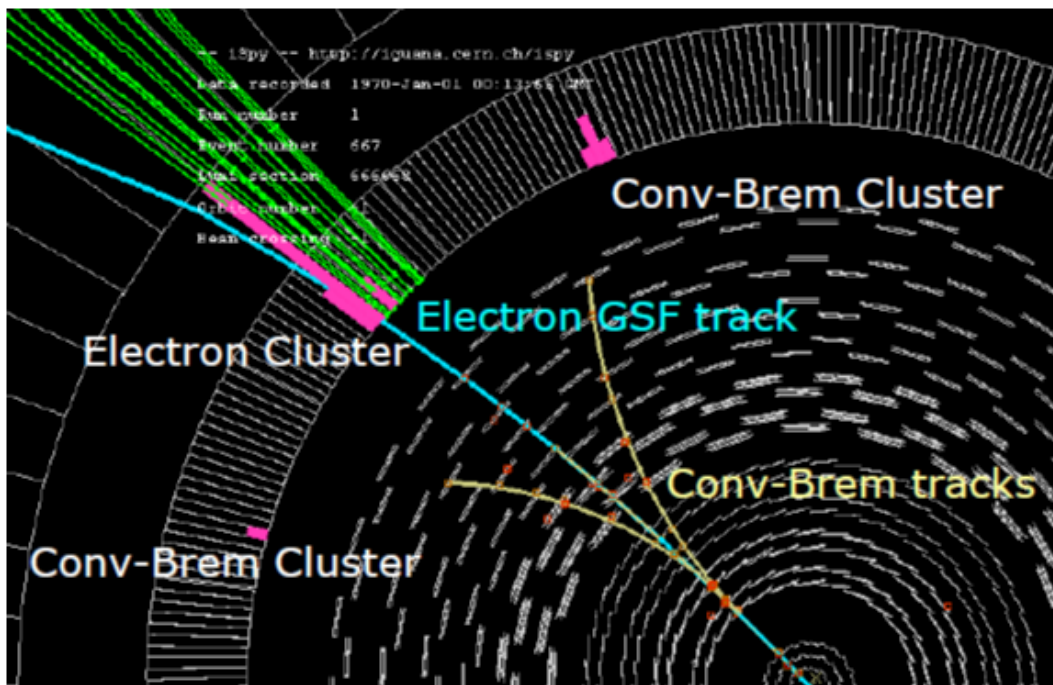
The electron can leave the energy to tracker and ECAL cluster. Due to electron's mass is very light, it can radiate some photon as bremsstrahlung radiation. It means that the electron will lose energy without charged tracks. To reconstruct the electron properly, it need to estimate the energy loss of the radiation. On CMS, Gaussian Sum Filter(GSF) was used to estimate track parameters by mixture of Gaussian distribution for each tracker layer.[4]

1. A track started from tracker based seed to ECAL PF cluster. This track was

## CHAPTER 6. PHYSICS OBJECT RECONSTRUCTION

recalculated by GSF method when the track reached to each layer.

2. Collect the energy of radiated photons to GSF track which are located at track's tangential direction.
3. When the GSF track is reached to ECAL, a "supercluster" energy can be collected to the electron candidate.



### 6.3 ParticleFlow(PF) algorithm

To maximize the efficiency performance of particle reconstruction, The "Particle-Flow"(PF) algorithm was developed. This algorithm links sub detector and another sub detector to recover particle efficiency. Especially, it can share the energy within a cell to multiple cluster. So, we can divide multiple particle from a overlapped energy deposit. On this study, the PF particles are used instead of standalone based ones.[5]

#### 6.3.1 Charged Hadron, Neutral Hadron and Photon

To separate Charged, neutral and photons from calorimeter hits, particle flow algorithm is used. This algorithm can provide some links about track-ECAL/track-HCAL/ECAL-HCAL/track-track/ECAL-preshower. If some hit successfully links to 2 or above PF elements(For example, track-HCAL and track-ECAL), the algorithm separate and share the energy from deposited hits to proper track. A Photon can not deposit the energy to tracker and HCAL. So, the photon can not link to other sub system and also can not make a PF Element. However, if some particles are overlapped at same point of the photon, it need to consider to share the energy to photon and neutral hadron. Almost case, no track to ECAL link is assumed to the photon.

When we find the reset of the block(Mixture of PF element) after removing

## CHAPTER 6. PHYSICS OBJECT RECONSTRUCTION

the photons, we can separate charged and neutral hadron particle using fraction of energy and momentum.

### 6.4 Jet

The QCD particles like as the quark and gluon can not stable due to color neutral property. Therefore, we can measure these QCD particles as jet object. We used the PF Jets for analysis which are clustered using PF candidates from above selection with Anti  $K_T$  jet finding algorithm.

#### 6.4.1 b-tagging

A bottom quark will be hadronized to B meson. Because the B mesons have long life time, it can deposit the energy to tracker as follow the track from primary vertex to another secondary vertex. Using this property, we can divide the b-jet or non b-jet. This job is called as "b-tagging". On CMS, Combined Secondary vertex method is used to determine b-tagging. Main issue of this method is to use secondary vertex and jet kinematics and those information can be trained by multivariate analysis tools.

## 6.5 Missing ET

A Missing ET(MET) can be assumed to neutrino which can not measure at CMS detector. So, we need to calculate missing ET, eta and phi to reconstruct the neutrino because of momentum conservation. We used the ParticleFlow MET(PF MET) for this analysis which are calculated using PF candidates.

## Chapter 7

# Reconstruction of the charmed mesons

On this analysis, to reconstruct the charmed meson is very important. Because, if we can not reconstruct precisely, its result has very large uncertainty. Therefore, we need to study how to reconstruct charmed meson and remove combinatory background from lack of information.

### 7.1 Track Selection

To reconstruct a charmed meson, we need to select proper tracks(or particle) from jet constituents. A particle flow jet included the daughters information when the jet was clustered from particle flow candidates. Therefore, we can acquire the tracks

## CHAPTER 7. RECONSTRUCTION OF THE CHARMED MESONS

from jet daughters. A daughter can be assigned to a charged hadron or neutral hadron and a lepton. To make vertex from 2 or 3 tracks which come from b-jet should be succeeded to remove ridiculous vertex.

### 7.1.1 Kalman vertex fitter

This vertex fitter is based on kalman filter which are used to reduce background using already known noise. Actually, this vertex fitter will work a global least-squares minimization from track to track. However, it can help to guess energy loss which come from multiple scattering and so on.

## 7.2 Reconstruction of charmed meson

On this analysis, we focus on  $J/\psi$ ,  $D^0$  and  $D^*$ (2010). Because, these mesons only have soft lepton and charged particle daughters. When the soft lepton are used, it can reduce combinatory background. As same words,  $D^{*0}$ (2007)  $\rightarrow D0 + \pi0$  and  $D^+ \rightarrow K0 + l + \nu$  are not used.

### 7.2.1 $J/\psi$

$$B^+ \rightarrow (J/\psi \rightarrow l^+l^-) + K^+ \quad (7.1)$$

$$B^0 \rightarrow (J/\psi \rightarrow l^+l^-) + K^+ + \pi^- \quad (7.2)$$

## CHAPTER 7. RECONSTRUCTION OF THE CHARMED MESONS

A  $J/\psi$  meson can be decayed to dilepton pair like as  $\mu^+\mu^-$  or  $e^+e^-$ . So, we can acquire very clean invariant mass shape using this meson. It was reconstructed by soft lepton pair among jet daughters. On this analysis, we only used  $pT > 4\text{GeV}/c$  muon pair to avoid misidentification. Below  $4\text{GeV}/c$  muon can not reach to muon system. Because this meson channel is very rare, it need to study to recover efficiency from uncertainty tracks.

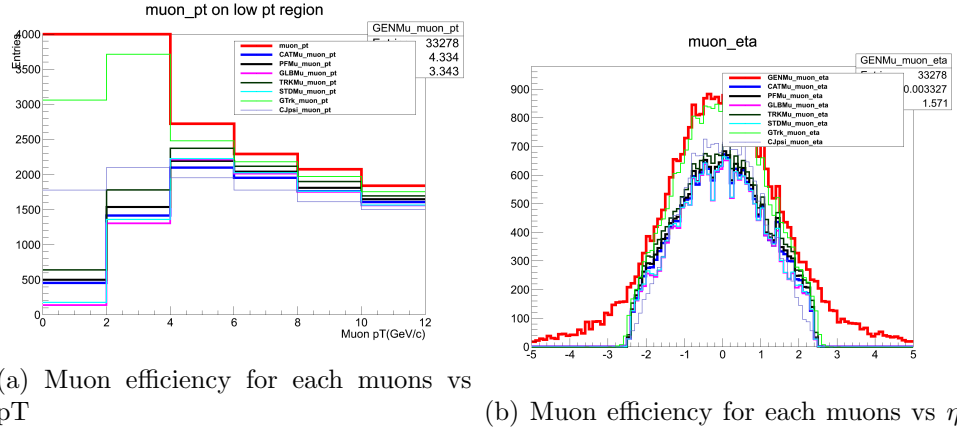
### 7.2.2 $D^0$

$$B^- \rightarrow (D^0 \rightarrow K^- + \pi^+) + l^- + \bar{\nu}_l \quad (7.3)$$

A  $D^0$  meson can be decayed to kaon and pion. However, we do not know that any charged hadron is a kaon or a pion. So, we assumed that all opposite sign pairs of charged hadron from jet daughters to kaon and pion. Then, the calculate the pair's invariant mass and cut with  $D^0$  mass window  $1.864 \pm 0.050\text{GeV}/c^2$ . A soft lepton tag can reduce combinatory background but the tag was not applied yet. Instead of soft lepton tag, we used  $L_{xy}$  and  $L_{3D}$  cut are applied. It help to remove which are too close to primary vertex. It means that that track did not come from b quark jets.

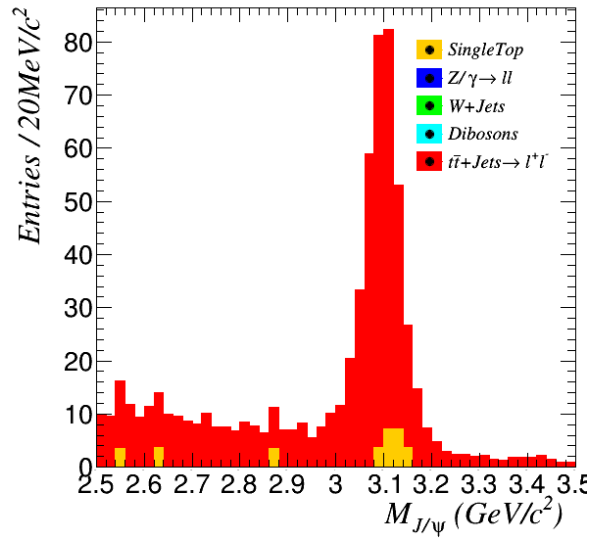


CHAPTER 7. RECONSTRUCTION OF THE CHARMED MESONS



(a) Muon efficiency for each muons vs pT

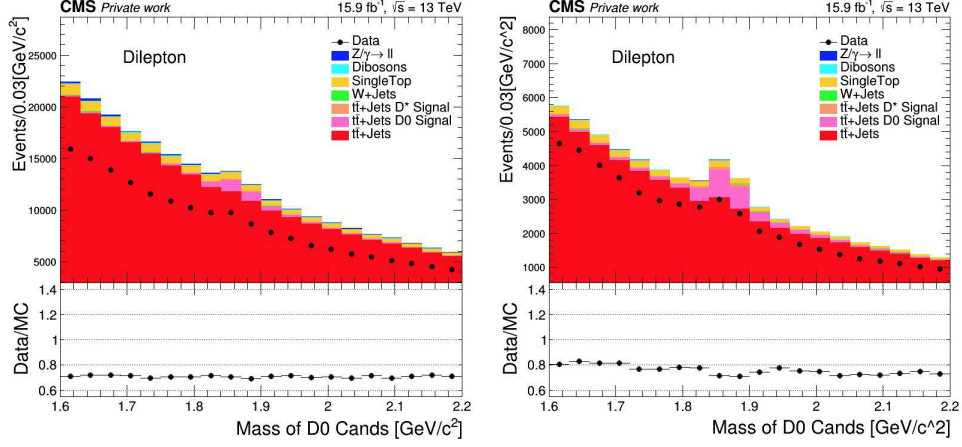
(b) Muon efficiency for each muons vs  $\eta$



(c)  $J/\psi$  mass distribution

Figure 7.1: Various muon reconstruction candidates properties and  $J/\psi$  mass distribution

## CHAPTER 7. RECONSTRUCTION OF THE CHARMED MESONS



(a) D0 invariant mass distribution with- (b) D0 invariant mass distribution with  
out optimized cut  $L_{XY}$  and  $L_{3D}$  cut

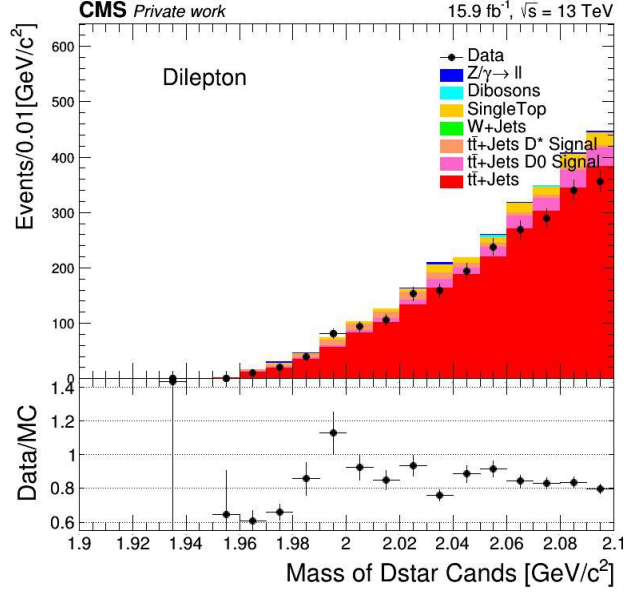
Figure 7.2: D0 Candidates invariant mass distribution

### 7.2.3 $D^*(2010)$

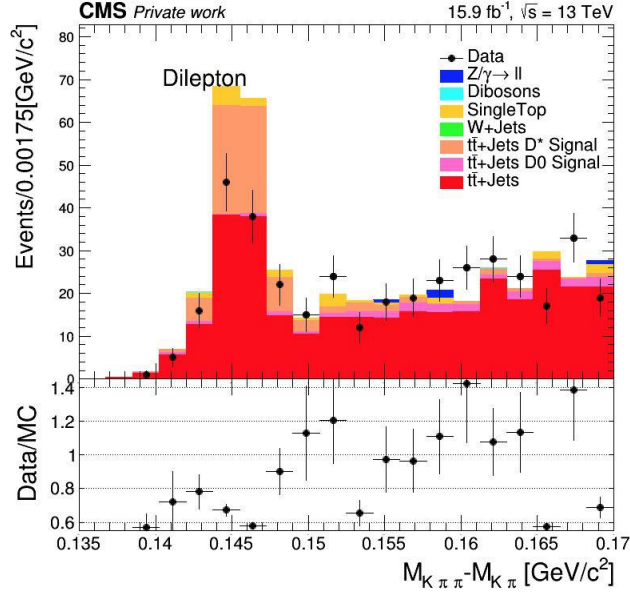
$$B^0 \rightarrow (D^{*+} \rightarrow D^0 + \pi^+ \rightarrow K^- + \pi^+ + \pi^+) + l^+ + \nu_l \quad (7.4)$$

$D^*(2010)$  meson can be decayed to D0 and pion. In this case, we can hope that D0 also will be decay to kaon and pion meson. It means that this  $D^*$  meson can be measured only by charged hadron particles like as D0. Differ from D0,  $D^{*\pm}(2010)$  meson's invariant mass can not measure directly due to other decay channel like as  $D^+$ . However, we can observed  $D^*$  meson using difference mass between  $D^*$  and its D0 mass. This difference mass distribution is more clean than D0 meson. So, this  $D^*$  meson also good candidate to measure top quark mass.

CHAPTER 7. RECONSTRUCTION OF THE CHARMED MESONS



(a)  $D^*$  candidates invariant mass distribution. On this plot,  $D^*$  can not separate from combinatory background.



(b)  $D^*$ - $D_0$  invariant difference mass distribution.

Figure 7.3:  $D^*$  Candidates invariant mass and difference mass distribution

## Chapter 8

# Top quark mass measurement

### 8.1 Monte Carlo Samples

The CMS data management group provided the central samples about MC simulation data. For  $t\bar{t}$  dileptonic decay channel events, we use proper datasets which can have 2 leptons or above. We used  $t\bar{t} \rightarrow l^+l^-$  samples which was generated by POWHEG generator at the next-to-leading order(NLO) in QCD.[6][7][8] This signal sample was tuned by underlying event as CUETP8M1[9] and PYTHIA8[10] was used for hadronization. For background, inclusive W process, drell-Yan, diboson(WW,WZ,ZZ) and single top tW channel were used. Those samples can decay to the dilepton or have a large cross section with 1 lepton. The inclusive W(W+Jets) sample was generated by aMC@NLO generator[11]. The drell-yan + additional jets(DYJets) was generated by aMC@NLO generator. The single top

## CHAPTER 8. TOP QUARK MASS MEASUREMENT

tW channel was generated by POWHEG generator for top and anti top quark. The diboson(VV) samples about WW, WZ and ZZ were generated by PYTHIA8. To avoid double counting between matrix element of real emission for NLO and parton shower, every multiple jet samples were applied MLM merging for Leading-Order and FFX merging for NLO was used. Every NLO samples were simulated by using NNPDF30\_NLO\_as.0118 which is a set of neural network parton distribution function of LHAPDF[12]. In addition, every LO samples were simulated using NNPDF30\_lo\_as.0130 pdf set. In addition, we also checked fast simulation by Delphes simulator for toy  $100fb^{-1}$  simulation using same dataset.

### 8.2 Collision Data

On this analysis, we used Run2016 collision data which is  $\sqrt{s}=13\text{TeV}$  and  $\mathcal{L} = 15.9fb^{-1}$ . Tab.8.2 shows a detail information for collision data. For each primary dataset were the mixture of High Level Trigger(HLT). For analysis, we used specific HLTs trigger from primary dataset at Tab.8.3 for each channel. In short,

- Double Mu : a Leading muon  $pT > 17\text{GeV}/c$  and 2nd leading muon  $pT > 8\text{GeV}/c$
- Double EG : a Leading electron  $pT > 17\text{GeV}/c$  and 2nd leading electron  $pT > 12\text{GeV}/c$

CHAPTER 8. TOP QUARK MASS MEASUREMENT

MC Sample	Cross section [pb]	luminosity [fb <sup>-1</sup> ]
DYJetsToLL_M-50_TuneCUETP8M1_13TeV-amcatnloFXFX-pythia8	6025.2	3.19
DYJetsToLL_M-10to50_TuneCUETP8M1_13TeV-amcatnloFXFX-pythia8	18610	1.21
WJetsToLNu_TuneCUETP8M1_13TeV-amcatnloFXFX-pythia8	61526.7	0.53
TT_TuneCUETP8M1_13TeV-powheg-pythia8	831.76	111.7
TT_TuneCUETP8M1_13TeV-powheg-scaleup-pythia8	831.76	11.94
TT_TuneCUETP8M1_13TeV-powheg-scaledown-pythia8	831.76	11.95
TT_TuneCUETP8M1_mt0p1695_13TeV-powheg-pythia8	903.82	32.31
TT_TuneCUETP8M1_mt0p1755_13TeV-powheg-pythia8	766.30	38.13
TT_TuneCUETP8M1noCR_13TeV-powheg-pythia8	831.76	29.31
TT_TuneCUETP8M1mpiOFF_13TeV-powheg-pythia8	831.76	29.09
TT_TuneEE5C_13TeV-powheg-herwigpp	831.76	23.80
ST_tW_top_5f_inclusiveDecays_13TeV-powheg-pythia8_TuneCUETP8M1	35.85	27.85
ST_tW_antitop_5f_inclusiveDecays_13TeV-powheg-pythia8_TuneCUETP8M1	35.85	27.48
WW_TuneCUETP8M1_13TeV-pythia8	118.7	8.36
WZ_TuneCUETP8M1_13TeV-pythia8	47.13	21.22
ZZ_TuneCUETP8M1_13TeV-pythia8	16.523	59.87

Table 8.1: Monte Carlo dataset list

CHAPTER 8. TOP QUARK MASS MEASUREMENT

Channel	Data Sample	Run Range	luminosity ( $fb^{-1}$ )
Double Muon	Run2016B	Run273150 275376	5.87
	Run2016C	Run275657 275783	2.65
	Run2016D	Run276315 276811	4.35
	Run2016E	Run276831 277420	3.05
Double EG	Run2016B	Run273150 275376	5.89
	Run2016C	Run275657 275783	2.65
	Run2016D	Run276315 276811	4.35
	Run2016E	Run276831 277420	3.05
Muon EG	Run2016B	Run273150 275376	5.87
	Run2016C	Run275657 275783	2.65
	Run2016D	Run276315 276811	4.35
	Run2016E	Run276831 277420	3.05

Table 8.2: Run2016 13TeV data  $\mathcal{L} = 15.9fb^{-1}$

Channel	Trigger
Double Muon	HLT Mu17 TrkIsoVVL Mu8 TrkIsoVVL DZ
	HLT Mu17 TrkIsoVVL TkMu8 TrkIsoVVL DZ
Double EG	HLT Ele17 Ele12 CaloIdL TrackIdL IsoVL DZ
Muon EG	HLT Mu17 TrkIsoVVL Ele12 CaloIdL TrackIdL IsoVL
	HLT Mu8 TrkIsoVVL Ele17 CaloIdL TrackIdL IsoVL

Table 8.3: High Level Trigger information for each primary datasets

- Muon EG : 1st leading muon  $pT > 17GeV/c$  and electron  $pT > 12GeV/c$  or  
1st leading electron  $pT > 17GeV/c$  and muon  $pT > 8GeV/c$

### 8.3 Event Selection

To reduce background events, we need to apply particle selection and kinematic event selection.

## CHAPTER 8. TOP QUARK MASS MEASUREMENT

### 8.3.1 Object selection

#### 8.3.1.1 Muon

- $pT > 20\text{GeV}/c$  and  $|\eta| < 2.4$
- $\chi^2/\text{ndof} < 10$  for global muon fit
- $\geq 1$  hit(s) at muon chamber
- $\geq 2$  matched station
- $> 5$  Number of of valid hits at inner tracker
- $< 0.15$   $\Delta\beta$  correction applied relative isolation within a cone size 0.4
- $d_{xy} < 0.2\text{cm}$  and  $d_z < 0.5\text{cm}$  with respect to the primary vertex to reduce the muons which are come from pileup or noise.

#### 8.3.1.2 Electron

- $pT > 20\text{GeV}/c$  and  $|\eta| < 2.4$  exclude  $1.4442 < |\eta_{\text{super cluster}}| < 1.566$  to avoid crack region.
- cus based medium ID described in Tab.8.4

#### 8.3.1.3 Jet

- $pT > 30\text{GeV}/c$  and  $|\eta| < 2.4$



CHAPTER 8. TOP QUARK MASS MEASUREMENT

Cut parameter	barrel region	endcap region
full5x5_sigmaIetaIeta <	0.0101	0.0283
abs( $\delta$ EtaIn) <	0.0103	0.00733
...	...	...

Table 8.4: Electron cut based medium ID

- Veto the ridiculous energy deposit jets like as only neutral or only charged particles jets. Detail in Tab 8.5.
- Veto jets which are too close with isolated lepton. ( $\Delta R < 0.4$ )

Cut parameter	value
Neutral Hadron Fraction	< 0.99
Neutral EM Fraction	< 0.99
Number of Constituent	> 1
Charged Hadron Fraction for barrel region	> 0
Charged Constituents for barrel region	> 0
Charged EM Fraction for barrel region	< 0.99

Table 8.5: Jet Loose ID

### 8.3.2 Kinematic selection

1. We skipped out if an event did not have 2 opposite electric charged leptons. This cut can rule out "Inclusive W" events from events. Also, we checked an invariant mass of dilepton is larger than  $20GeV/c^2$  due to removal like as prompt  $J\psi$  and QCD resonance events.
2. The Drell-yan process is a major background of dilepton channel. We can

## CHAPTER 8. TOP QUARK MASS MEASUREMENT

reduce this process by the z mass veto cut which are dilepton's invariant mass cut around Z boson( $91 \pm 15 GeV/c^2$ ).

3. The number of jet is very important property of  $t\bar{t}$  events. We required 2 jets at least. It can reduce diboson, drell-yan and single top process.
4. On  $t\bar{t}$  events, two neutrinos are generated from W boson. It can not directly measured but we can confirm the Missing ET for these neutrino. We used  $MET > 40 GeV$  cut for this analysis because we selected the lepton minimum pT as  $20 GeV/c^2$  because of the high level triggers(HLTs).
5. On this analysis, we need to find a b-tagged jet at least. Because, the b-tagging efficiency is about 70%.[13] To require 2 b-jets is too tight for this analysis.

Event selections	Nb of MC events (in thousands)	Expected Nb. of Events for $16 fb^{-1}$
$t\bar{t} \rightarrow (W^+b)(W^-\bar{b}) \rightarrow (l^+\nu + b) + (l^-\bar{\nu} + \bar{b})$	104,573 k	k
Dilepton mass ( $M_{ll} > 20$ GeV)	16,989 k	k
Z veto ( $M_{ll} < 76$ GeV or $M_{ll} > 106$ GeV)	12,401k	k
Jet requirements ( $N_{jets} > 2$ )	8,759 k	k
Missing Transverse Energy ( $E_T^{miss} > 40$ GeV )	6,519 k	k
b-jet tagging ( $N_{b-jets} > 1$ )	5,410 k	k

Table 8.6: Event Selection for dileptonic decay channel for ttbar signal sample.

## CHAPTER 8. TOP QUARK MASS MEASUREMENT

Dataset name	Nb. of expected events	Percentage (%)
$t\bar{t} \rightarrow (W^+b)(W^-\bar{b}) \rightarrow (l^+\nu + b) + (l^-\bar{\nu} + \bar{b})$	?	94.39
Single top	?	4.44
Drell-Yan + jets	?	1.02
W + jets	?	0.0
WW	?	0.12
WZ	?	0.02
ZZ	?	0.01

Table 8.7: The expected numbers of signal events and backgrounds after event selection

### 8.4 Systematic Errors

The systematic errors are come from various limitation of measure using this method.

We can measure various errors and list up to Tab.8.8 for D0 case.

- Choice of renormalization( $\mu_R$ ) and factorization scale( $\mu_F$ ) :  $\mu_R$  and  $\mu_F$  are related to jet multiplicity. These parameter usually are handle by Q factor where  $Q^2 = m_t^2 + \sum(p_T^{\text{parton}})^2$ . On this analysis,  $\mu_R=\mu_F=2Q$  or  $Q/2$  are used.
- Hadronization model : On this error calculation, A PYTHIA8 generator is used for hadronization for ttbar sample. PYTHIA8 generator is based on Lund fragmentation model which is assumed string model between QCD particles. To calculate this error, we compared PYTHIA8 dataset with Herwigpp one.
- Underlying Event(Multi Parton Interaction only) : A different UE tune sam-

## CHAPTER 8. TOP QUARK MASS MEASUREMENT

ples is not generated now. So, we can only use  $t\bar{t}$  no MPI sample to measure MPI effect for mass measurement.

- Color reconnection : This error can affect to b fragmentation. So, it need to measure to calculate systematic errors. We used a dedicated sample which do not have color reconnection among QCD particles.
- Top Quark Pt : When someone measure differential ttbar production cross section, they found pT spectrum was softer than estimated. We applied top pT weight value to event-by-event but it has an uncertainty. So, we need to compare top pT weighted one and not weighted sample.
- Jet energy scale and jet energy resolution : On this analysis, jet energy can not affect directly to measure top quark mass. However, our selection for tracks started from jet's daughter. It means that the jet energy scale and resolution can affect jet finding and also affect track looping. We check the JES and JER separately by using up and down uncertainty case.
- Lepton energy scale : A lepton distribution between MC and real data always can not agree. So, we need to apply the weight for each lepton's pT and eta. This weight can have an uncertainty because of energy resolution of pT. So, we need to check lepton energy scale's up and down uncertainties.

CHAPTER 8. TOP QUARK MASS MEASUREMENT

Source	$\Delta m_t [\text{GeV}]$	
Theoretical uncertainties		
$\mu_R/\mu_F$ scales $t\bar{t}$	-2.97	5.05
Hadronization model	7.08	
Underlying event	2.30	
Color reconnection	1.00	
Top quark $p_T$	-3.12	
Total theoretical uncertainties	-8.66	9.57
Experimental uncertainties		
Jet energy scale	0.69	-0.17
Jet energy resolution	0.11	0.15
Lepton energy scale	-0.50	0.52
Total experimental uncertainties	-0.86	0.57
Total systematic uncertainties	-8.69	9.57
Statistical uncertainties	$\pm 5.73$	

Table 8.8: Systematic errors for D0 case

## CHAPTER 8. TOP QUARK MASS MEASUREMENT

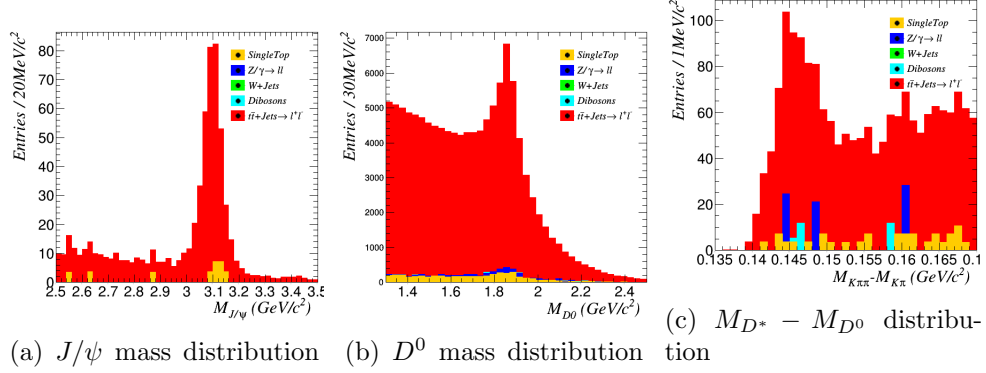


Figure 8.1: Reconstructed charmed meson mass distribution

## 8.5 Result

### 8.5.1 Fast Simulation result for toy $100fb^{-1}$

Before to measure top quark mass from Run2016 data, we studied fastSim simulation using Delphes for  $100fb^{-1}$ . We acquired invariant mass of lepton and charmed meson. Detail for Fig8.1, Fig8.2, Fig8.3 and Fig8.4. Finally, we can acquired how much sensitive for each meson from calibration curve. Please, see Fig8.5 for detail.

### 8.5.2 Full Simulation result for Run2016

For CMS Run2016 data, we can acquired the  $D^0$  meson from Secondary vertex from jet's daughters.

CHAPTER 8. TOP QUARK MASS MEASUREMENT

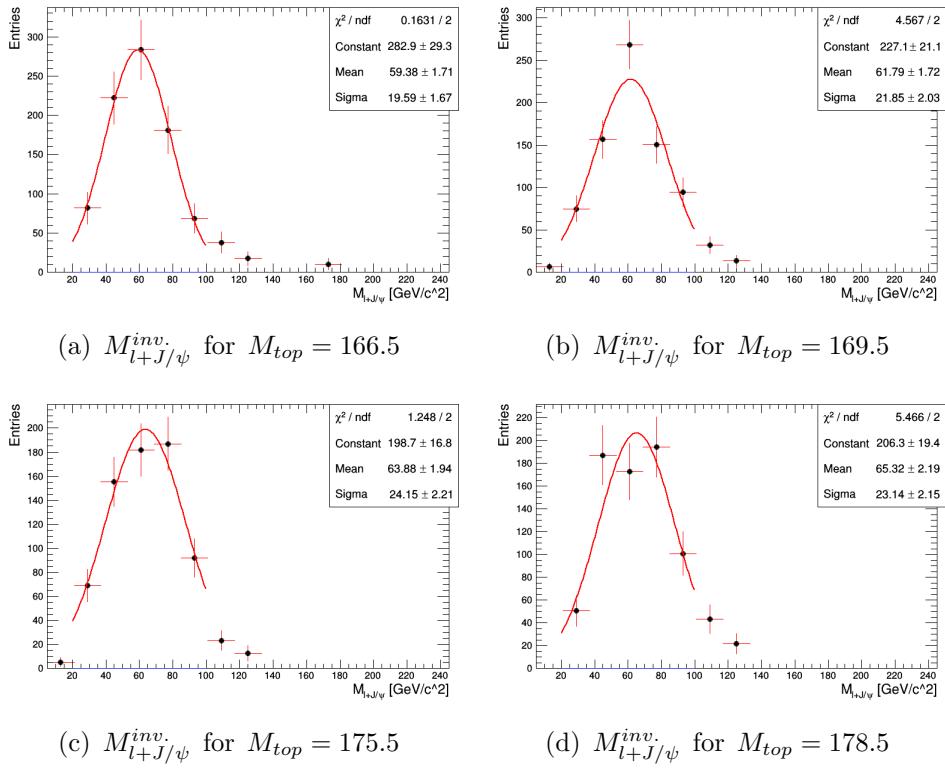


Figure 8.2:  $M_{l+J/\psi}^{inv.}$  with Gaussian fitting

CHAPTER 8. TOP QUARK MASS MEASUREMENT

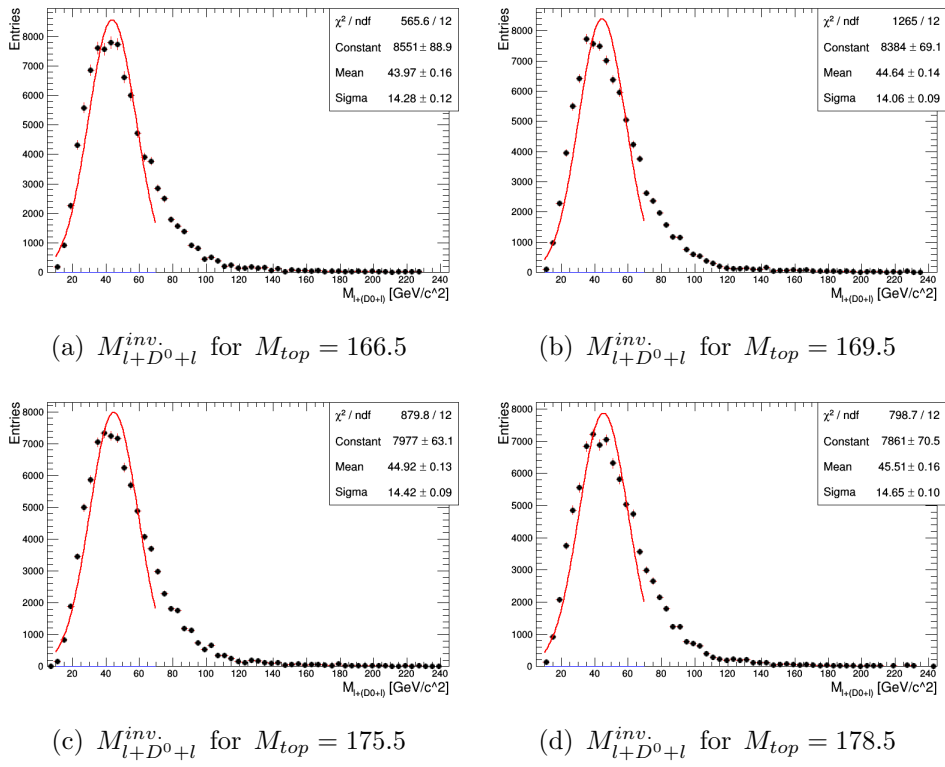


Figure 8.3:  $l + D^0 + l$  with Gaussian fitting



CHAPTER 8. TOP QUARK MASS MEASUREMENT

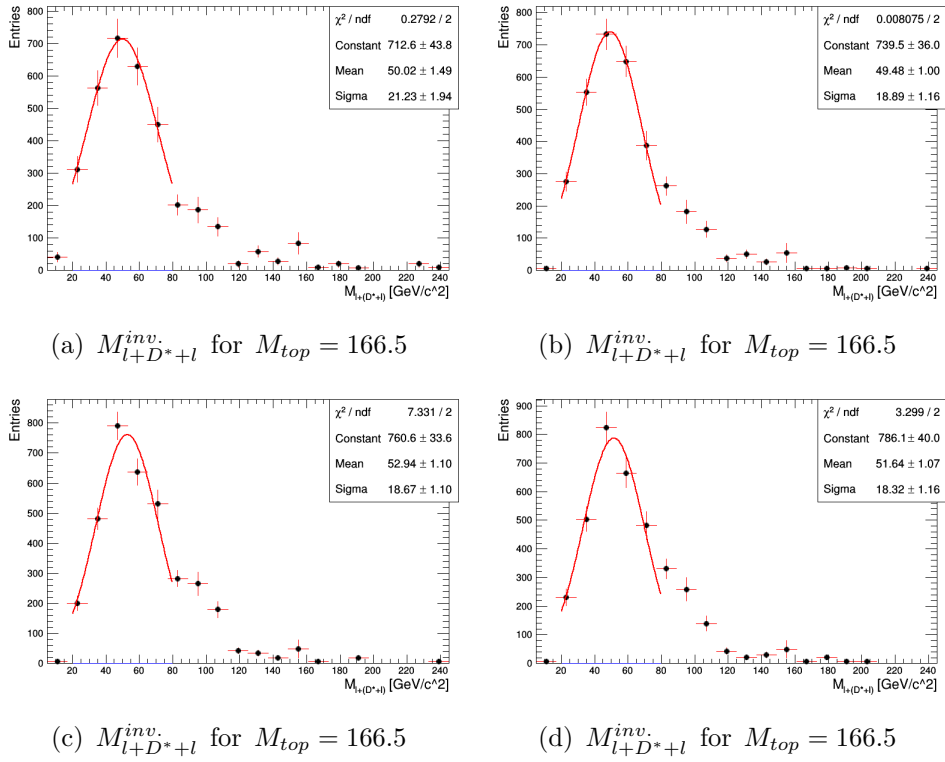


Figure 8.4:  $l + D^*(2010) + l$  with Gaussian fitting

CHAPTER 8. TOP QUARK MASS MEASUREMENT

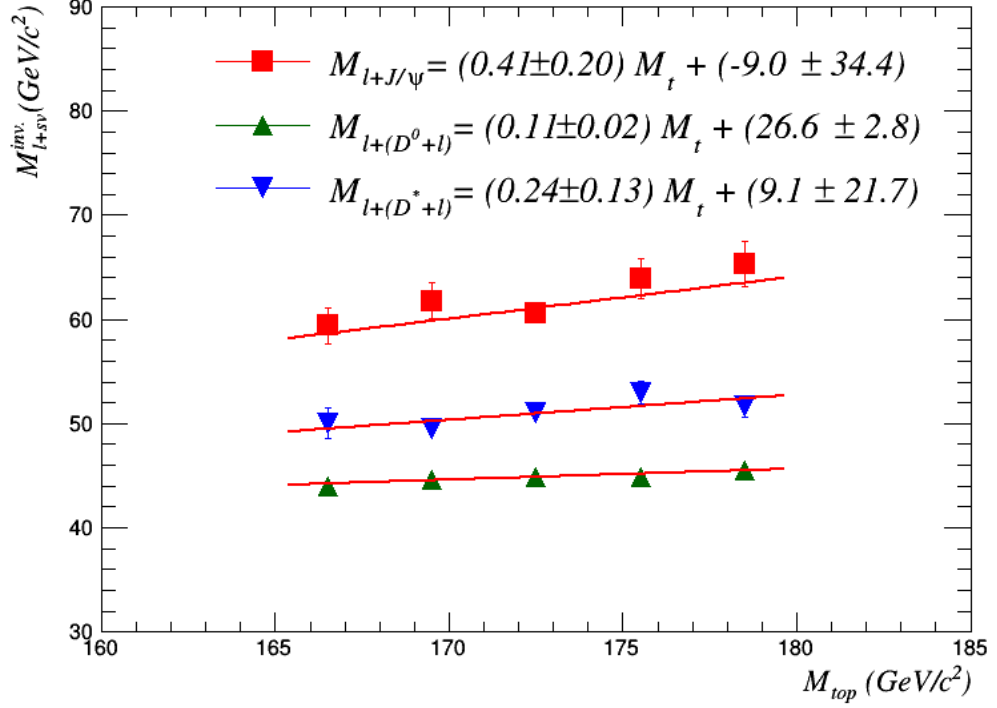


Figure 8.5: Calibration curve for fast simulation  $\mathcal{L} = 100 fb^{-1}$  at  $\sqrt{s} = 13 TeV$

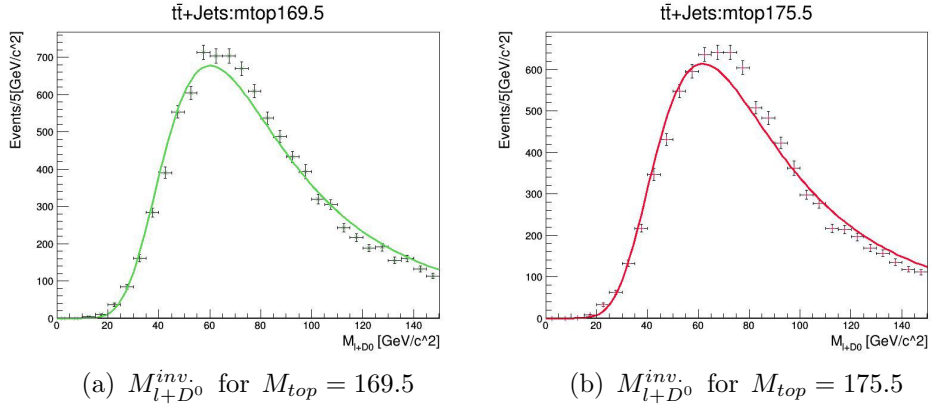


Figure 8.6:  $l + D^0$  with landau fitting

CHAPTER 8. TOP QUARK MASS MEASUREMENT

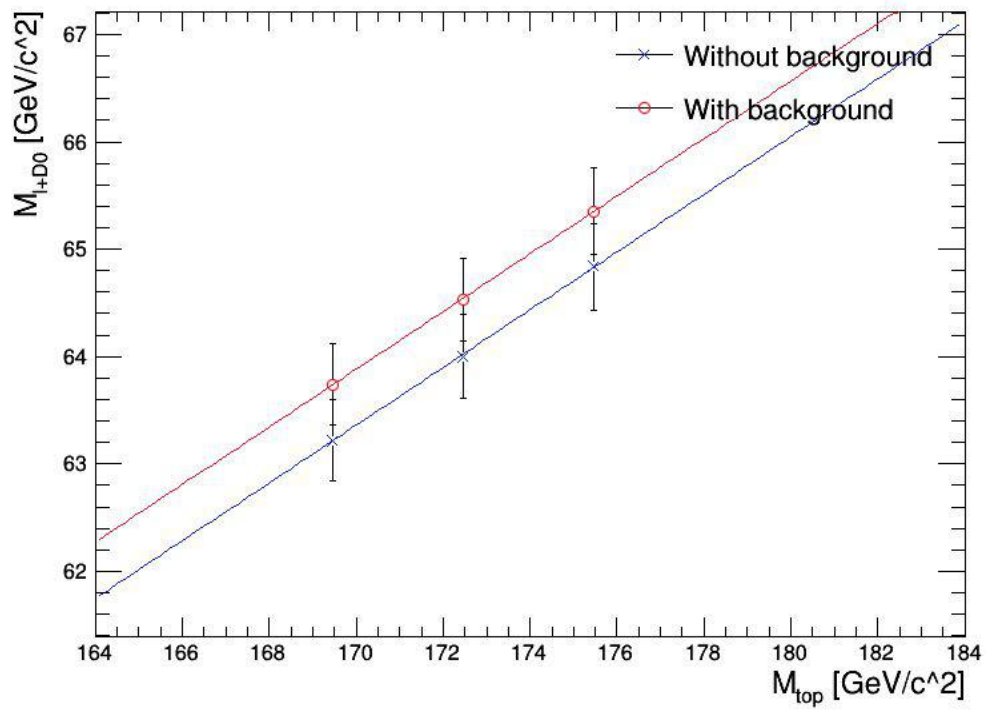


Figure 8.7: Calibration curve for full simulation  $\mathcal{L} = 15.9fb^{-1}$  at  $\sqrt{s} = 13TeV$

## Chapter 9

# Conclusion

In summary, we measured the top quark mass using invariant mass of lepton and charmed meson within b-jet. On fast simulation result with  $100fb^{-1}$  13TeV toy MC data, we acquired which meson is more sensitivity of top quark mass changes. In short,  $M_{l+J/\psi}$  has a slope by  $0.41 \pm 0.2$ . It is a highest slope among mesons which are researched. However, it has a large error bar due to statics. Instead of  $J/\psi$ ,  $D^0$  has completely opposite property. It has enough entries to draw shape stably. However, it has very large combinatory background. So, the invariant mass of lepton and D0 distribution has a landau shape instead of gaussian. In addition,  $D^*(2010)$  is average between  $J/\psi$  and  $D^0$ . Using Run2016  $15.9fb^{-1}$  13TeV data, we got the top quark mass using invariant mass of lepton and D0 meson.  $J/\psi$  and  $D^*(2010)$  can not be fitted stably due to lack of statics. The measured top quark

## CHAPTER 9. CONCLUSION

mass is  $180.69 \pm 5.73$  (stat.)  $^{+9.61}_{-8.67}$  (syst.)  $GeV/c^2$ . Its value agrees already known top quark mass. This method has a merit about the jet energy uncertainty. Its value is about  $0.8GeV/c^2$ . However, it has a limitation about statics and systematic errors. We can't not overcome about static errors but systematic errors can be improved to study to remove combinatory background in order to increase a slope of calibration curve.

# Reference

- [1] C. Patrignani et al. Review of Particle Physics. *Chin. Phys.*, C40(10):100001, 2016.
- [2] Kevin Lannon, Fabrizio Margaroli, and Chris Neu. Measurements of the production, decay and properties of the top quark: a review. *The European Physical Journal C*, 72(8):2120, 2012.
- [3] The CMS collaboration. Particle-flow commissioning with muons and electrons from J/Psi and W events at 7 TeV. Technical Report CMS-PAS-PFT-10-003, CERN, 2010. Geneva, 2010.
- [4] Vardan Khachatryan et al. Performance of Electron Reconstruction and Selection with the CMS Detector in Proton-Proton Collisions at  $\sqrt{s} = 8$  TeV. *JINST*, 10(06):P06005, 2015.
- [5] Florian Beaudette. The CMS Particle Flow Algorithm. In *Proceedings, International Conference on Calorimetry for the High Energy Frontier (CHEF*

## REFERENCE

- 2013): Paris, France, April 22-25, 2013, pages 295–304, 2013.
- [6] Paolo Nason. A New method for combining NLO QCD with shower Monte Carlo algorithms. *JHEP*, 11:040, 2004.
- [7] Stefano Frixione, Paolo Nason, and Carlo Oleari. Matching NLO QCD computations with Parton Shower simulations: the POWHEG method. *JHEP*, 11:070, 2007.
- [8] Simone Alioli, Paolo Nason, Carlo Oleari, and Emanuele Re. A general framework for implementing NLO calculations in shower Monte Carlo programs: the POWHEG BOX. *JHEP*, 06:043, 2010.
- [9] CMS Collaboration. Event generator tunes obtained from underlying event and multiparton scattering measurements. *The European Physical Journal. C, Particles and Fields*, 76, 2016.
- [10] Torbjorn Sjostrand, Stephen Mrenna, and Peter Z. Skands. A Brief Introduction to PYTHIA 8.1. *Comput. Phys. Commun.*, 178:852–867, 2008.
- [11] J. Alwall, R. Frederix, S. Frixione, V. Hirschi, F. Maltoni, O. Mattelaer, H.-S. Shao, T. Stelzer, P. Torrielli, and M. Zaro. The automated computation of tree-level and next-to-leading order differential cross sections, and their matching to parton shower simulations. *Journal of High Energy Physics*, 2014(7):1–157, 2014.

## REFERENCE

- [12] Andy Buckley, James Ferrando, Stephen Lloyd, Karl Nordström, Ben Page, Martin Rufenacht, Marek Schönherr, and Graeme Watt. LHAPDF6: parton density access in the LHC precision era. *Eur. Phys. J.*, C75:132, 2015.
- [13] Serguei Chatrchyan et al. Identification of b-quark jets with the CMS experiment. *JINST*, 8:P04013, 2013.



## 국문초록

탑 쿼크의 질량을 정밀하게 측정하는 것은 이후 힉스와 같은 붕괴모드를 거쳐가는 입자들의 질량을 보다 더 정밀하게 측정하게 해주며 이론적으로 알려져 있는 문제들을 해결하기 위해 필수적으로 노력해야 하는 연구이다. 현재 탑쿼크의 질량 정밀도는 매우 높은 수준이며 이를 더욱 개선하기 위한 여러가지 방법들이 제안되고 있다.

여러가지의 측정 법 중 탑-반탑쿼크의 생성사건에서 생겨난 b제트에서 참 중간자들을 재구성하여 탑 쿼크의 질량을 측정하는 방법 또한 제안되었다. 이 방법은 사용되는 입자들 중에 b제트의 에너지를 직접적으로 사용하지 않기 때문에 앞으로 더욱 커질 수밖에 없는 동시충돌 사건 같이 제트의 에너지 불확실성 증가시킬 수 있는 문제를 피해갈 수 있을 것으로 기대되고 있다.

이 연구에서는 2016년 LHC에서 획득된  $15.9fb^{-1}$  크기의 데이터를 이용하여 참 중간자 입자들을 재구성한 후 이를 모의실험을 통해 계산된 탑 쿼크의 질량과 비교하여 봄으로써 실제 탑 쿼크의 질량이 어떻게 찾아지는지를 조사하였다. 이를 통하여 탑쿼크의 질량을 D0중간자를 통하여 획득하였다. 최대한 확인 가능한 계통오차를 포함한 결과는  $180.69 \pm 5.73$  (stat.)  $^{+9.61}_{-8.67}$  (syst.)  $GeV/c^2$ 이다.

**주요어휘:** LHC, CMS, 탑 쿼크,  $J/\psi$  중간자

## 감사의 글

이후 작성 예정입니다.